

Theoretical mass estimates for the Mira-type variable R Hydrae

Yu. A. Fadeyev*

*Institute of Astronomy, Russian Academy of Sciences, Pyatnitskaya ul. 48, Moscow, 119017
Russia*

Received April 4, 2023; revised April 27, 2023; accepted April 27, 2023

Abstract — Calculations of stellar evolution at initial abundances of helium $Y = 0.28$ and heavier elements $Z = 0.014$ were done for stars with masses on the main sequence $1.7M_{\odot} \leq M_{\text{ZAMS}} \leq 5.2M_{\odot}$. Evolutionary sequences corresponding to the AGB stage were used for modelling the pulsation period decrease observed for almost two centuries in the Mira-type variable R Hya. Diminution of the period from $\Pi \approx 495$ d in the second half of the eighteenth century to $\Pi \approx 380$ d in the 1950s is due stellar radius decrease accompanying dissipation of the radiation–diffusion wave generated by the helium flash. For all the history of its observations R Hya was the fundamental mode pulsator. The best agreement with observations is obtained for eight evolutionary models with initial mass $M_{\text{ZAMS}} = 4.8M_{\odot}$ and the mass loss rate parameter of the Blöcker formula $0.03 \leq \eta_{\text{B}} \leq 0.07$. Theoretical mass estimates of R Hya are in the range $4.44M_{\odot} \leq M \leq 4.63M_{\odot}$, whereas the mean stellar radius ($421R_{\odot} \leq \bar{R} \leq 445R_{\odot}$) corresponding to the pulsation period $\Pi \approx 380$ agrees well with measurements of the angular diameter by methods of the optical interferometric imaging.

Keywords: *stellar evolution; stellar pulsation; stars: variable and peculiar*

INTRODUCTION

The variable star R Hya belongs to the long-period Mira-type pulsating variables (Samus' et al. 2017) and its first observations were made by Jan Heweliusz in 1662 and Geminiano Montanari in 1670 (Hoffleit 1997; Zijlstra et al. 2002). However systematic observations of R Hya were conducted only since the second half of the XIXth century. A particular attention to this star was paid after detection of a rapid decrease in the period of its light variations (Schmidt 1865; Chandler 1882; Gould 1882; Cannon and Pickering 1909; Ludendorff 1916; Nielsen 1926; Müller 1929). The most comprehensive review of R Hya period change is given by Zijlstra et al. (2002). According to these data the onset of R Hya period decrease corresponds to the second half of the XVIIIth century when the star oscillated with period $\Pi \approx 495$ d. Since the end of the XVIIIth century the period decreased nearly linearly with the rate $\dot{\Pi} \approx -0.58$ d/yr and the period decline ceased in ≈ 1950 when the star oscillated with period $\Pi \approx 380$ d.

Detection of absorption lines of the unstable radioactive element technetium with a half-life $\tau \lesssim 2 \times 10^5$ yr in the spectrum of R Hya (Orlov and Shavrina 1984; Little et al. 1987; Lebzelter

*E-mail: fadeyev@inasan.ru

and Hron 2003) gives a good indication that this late-type pulsating variable is the asymptotic giant branch (AGB) star undergoing the thermal flash of the helium burning shell accompanied by the change of the surface chemical composition due to the third dredge-up. At the same time one should note that R Hya is in the early TP-AGB stage since this star is classified as the oxygen-rich Mira-type variable (Merrill 1946, 1957; Maehara 1971). The higher abundance of oxygen in comparison with carbon is also demonstrated by observations of maser emission of molecules OH (Lewis et al. 1995), H₂O (Takaba et al. 2001) and SiO (Humphreys et al. 1997).

Rough estimates based on evolutionary computations (Wood and Zarro 1981) show that the pulsation period change observed in R Hya is due to decrease of the stellar radius and luminosity after the maximum of the thermal flash in the helium burning shell. Unfortunately, the mass of the Mira-type variable R Hya remains still uncertain because a thorough analysis based on results of nonlinear stellar oscillations has not been done yet.

At present R Hya is the only Mira-type variable with the known duration of the period decrease ($170 \text{ yr} \lesssim \Delta t \lesssim 200 \text{ yr}$) as well as with the known values of the period at the onset ($\Pi_a^* \approx 495 \text{ d}$) and at the end ($\Pi_b^* \approx 380 \text{ d}$) of this interval (Zijlstra, 2002). In our previous paper (Fadeyev 2022) we have shown that analysis of the secular period change during the thermal flash of the Mira-type variable T UMi allowed us to obtain the reliable estimate of the stellar mass using the consistent evolutionary and nonlinear stellar pulsation calculations. Below we describe the results of similar calculations aimed at evaluating the mass M and the radius R of R Hya. The models of R Hya computed in the present study are tested by comparison of theoretical estimates of the mean stellar radius \bar{R} with results of angular stellar diameter measurements obtained by methods of the optical interferometry (Haniff et al. 1995; Ireland 2004; Woodruff et al. 2008).

EVOLUTIONARY SEQUENCES OF AGB STARS

The results presented below are based on evolutionary computations of stars from the main sequence up to the end of the AGB stage. We considered the stars with initial masses $1.7M_{\odot} \leq M_{\text{ZAMS}} \leq 5.2M_{\odot}$ and the initial helium abundance $Y = 0.28$. The initial metallicity (i.e. the abundance of elements heavier than helium) was assumed to be the same as the solar metallicity $Z = 0.014$ (Asplund 2009).

The evolutionary sequences were calculated with the program MESA version r15140 (Paxton et al. 2019). Convective mixing was treated according to Böhm-Vitense (1958) with mixing length to pressure scale height ratio $\alpha_{\text{MLT}} = 1.8$. Additional mixing at boundaries of convection zone was taken into account by using the prescription of Herwig (2000) with values of the overshooting parameter f_{ov} recommended by Pignatari et al. (2016). In particular, evolutionary stages before AGB were computed with $f_{\text{ov}} = 0.014$ whereas during the AGB phase the

overshooting parameter at the inner boundary of the outer convection zone was assumed to be $f_{\text{ov}} = 0.126$. Assumption on extended overshooting at the bottom of the outer convection zone provides a better agreement with carbon and oxygen abundances observed in AGB stars (Herwig et al. 2003; Pignatari et al. 2016). The rates of nuclear reactions and nucleosynthesis were calculated using the JINA Reaclib data base (Cyburt et al. 2010).

Evolutionary phases prior to the AGB (i.e. when the central helium abundance is $Y_c > 10^{-4}$) were computed with mass loss rates prescribed by the Reimers formula (Reimers 1975) with parameter $\eta_R = 0.5$, whereas evolution of AGB stars was computed according to Blöcker (1995) with parameter of the Blöcker formula $\eta_B = 0.05$. Additional calculations with mass loss parameters $\eta_B = 0.03$ and $\eta_B = 0.07$ were carried out for evolutionary sequences that showed a good agreement with observations of R Hya. In general we computed several dozen evolutionary sequences and then selected models of these sequences were used as initial conditions in hydrodynamic calculations for determination of the pulsation period.

The pulsation period and the stellar radius relate as $\Pi \propto R^{3/2}$ so that the temporal dependence of the pulsation period after the maximum of the helium shell luminosity $L_{3\alpha}$ can be obtained from that of the radius without time consuming hydrodynamic computations. Fig. 1 shows variation with time during the ninth thermal flash ($i_{\text{TP}} = 9$) of the stellar radius R in the star with mass $M = 1.96M_\odot$ (the evolutionary sequence $M_{\text{ZAMS}} = 2M_\odot$, $\eta_B = 0.05$). A similar plot for the star with mass $M = 4.21M_\odot$ (the evolutionary sequence $M_{\text{ZAMS}} = 4.5M_\odot$, $\eta_B = 0.05$) during the seventh thermal flash ($i_{\text{TP}} = 7$) is shown in Fig. 2. In both Figs. 1 and 2 the time t is set to zero at the maximum of $L_{3\alpha}$ and the maxima of $L_{3\alpha}$ are marked by filled circles with label 0.

At maximum of $L_{3\alpha}$ the gas in the hydrogen burning shell adiabatically expands so that the rate of energy release in the CNO cycle abruptly drops whereas outer layers of the star contract due to the lack of hydrostatic equilibrium. Decrease of the stellar radius and luminosity ceases at t_1 when the radiation diffusion wave generated by the helium flash reaches the bottom of the outer convection zone. Therefore, the time interval $\Delta t_{01} = t_1 - t_0$ is nearly the radiation diffusion time between the helium burning shell and the outer layers of the star. As seen in Figs. 1 and 2 the time interval Δt_{01} decreases with increasing stellar mass. Duration of the second phase of radius decrease ($\Delta t_{23} = t_3 - t_2$) exceeds the time interval Δt_{01} by more than an order of magnitude but also decreases with increasing stellar mass.

As seen in Figs. 1 and 2, the time intervals for stellar masses $M = 1.96M_\odot$ ($\Delta t_{01} = 206$ yr) and $M = 4.21M_\odot$ ($\Delta t_{23} = 226$ yr) are nearly the same and are close to the time interval ($170 \text{ yr} \lesssim \Delta t \approx 200 \text{ yr}$) of period decrease observed in R Hya. Therefore, in order to compute the model of the Mira-type variable R Hya we have to consider both phases of stellar radius decrease.

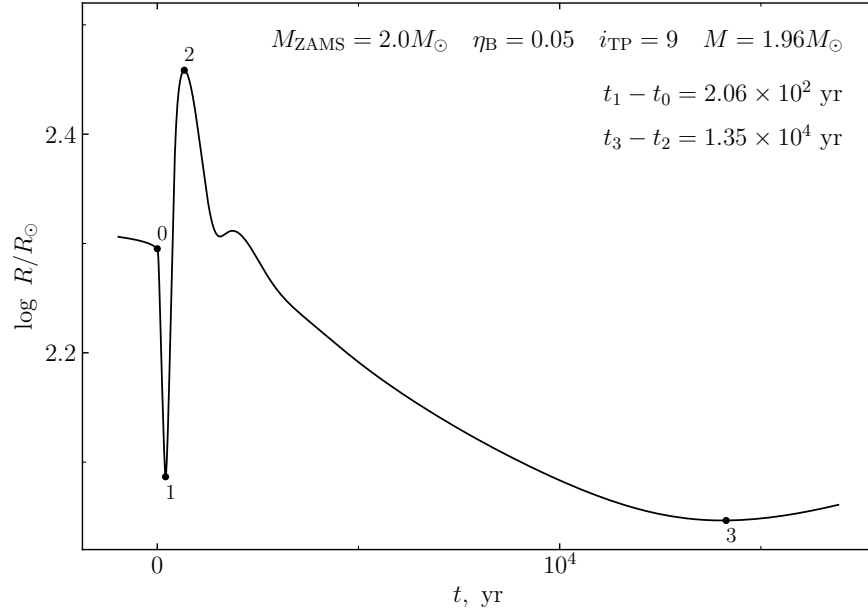


Figure 1. Radius variation of the star with mass $M = 1.96M_{\odot}$ (evolutionary sequence $M_{\text{ZAMS}} = 2.0M_{\odot}$, $\eta_{\text{B}} = 0.05$) during the thermal flash $i_{\text{TP}} = 9$. Evolutionary time t is set to zero maximum of $L_{3\alpha}$.

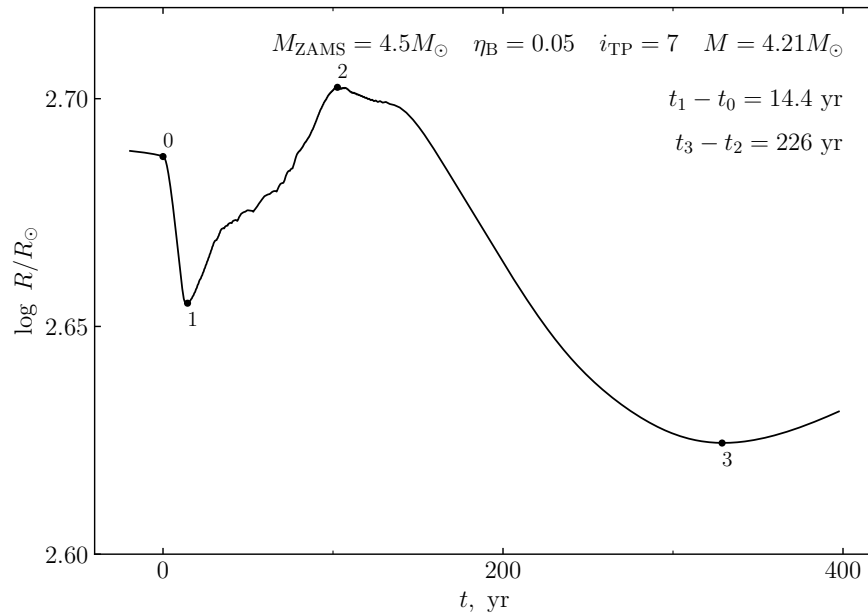


Figure 2. Same as Fig. 1 but for the star with mass $M = 4.21M_{\odot}$ (evolutionary sequence $M_{\text{ZAMS}} = 4.5M_{\odot}$, $\eta_{\text{B}} = 0.05$) during the thermal flash $i_{\text{TP}} = 7$.

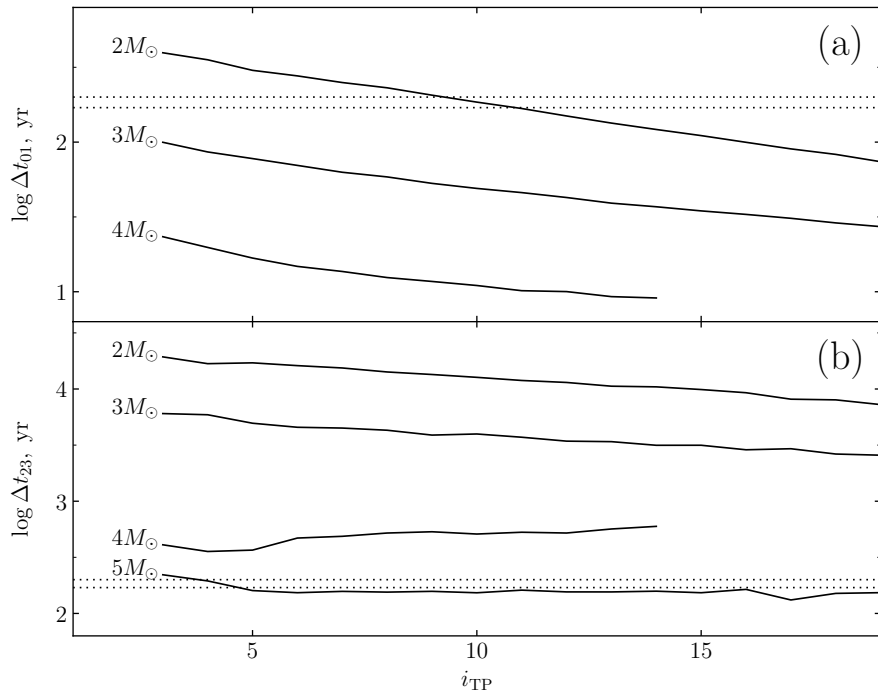


Figure 3. Duration of the first (a) and the second (b) phases of radius decrease as a function of the thermal flash serial number i_{TP} for evolutionary sequences calculated with $\eta_{\text{B}} = 0.05$. The initial masses M_{ZAMS} are given at the curves. Dotted lines show the time intervals 170 and 200 yr.

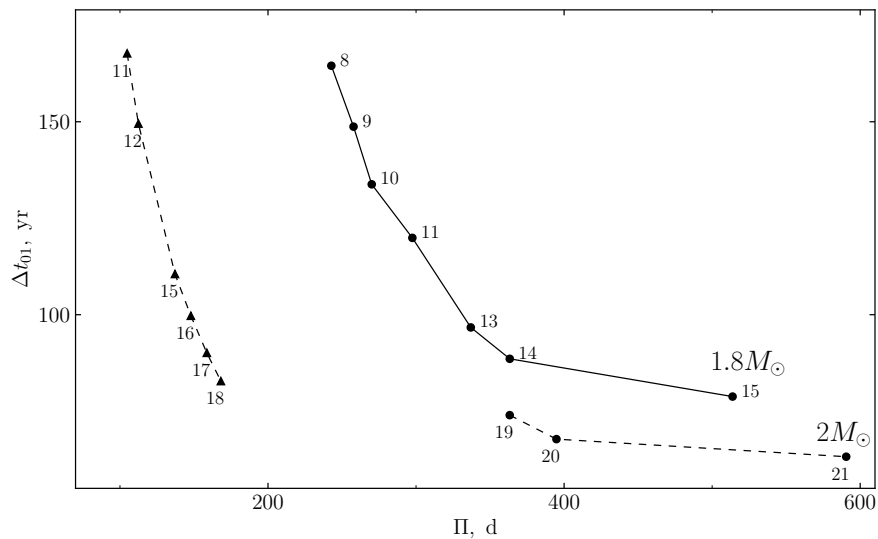


Figure 4. The diagram period Π – duration of the first phase of radius decrease Δt_{01} for evolutionary sequences $M_{\text{ZAMS}} = 1.8M_{\odot}$ (solid line) and $M_{\text{ZAMS}} = 2M_{\odot}$ (dashed line). Filled circles and triangles show the fundamental mode and the first overtone pulsators. The numbers at the curves show the serial number of the thermal flash i_{TP} .

The time interval of radius decrease depends not only on the stellar mass but also on the star age of the AGB star. This is illustrated in Fig. 3, where the time intervals Δt_{01} and Δt_{23} are shown as a function of the serial number of the thermal flash i_{TP} for several evolutionary sequences with initial masses $2M_{\odot} \leq M_{\text{ZAMS}} \leq 5M_{\odot}$. As seen in the plots, the time interval Δt_{01} is rather close to the observed value for the early AGB stage ($i_{\text{TP}} < 10$) in evolutionary sequences with initial masses $M_{\text{ZAMS}} < 3M_{\odot}$. The duration of the second phase of radius decrease Δt_{23} is close to observations in wider ranges of the serial number of the thermal flash ($i_{\text{TP}} > 5$) but for evolutionary sequences with higher initial masses: $4M_{\odot} < M_{\text{ZAMS}} \lesssim 5M_{\odot}$. To draw a more certain conclusion about applicability of the first or the second phase of radius decrease we have to evaluate the pulsation periods Π_0 and Π_2 at the onset of the radius diminution.

HYDRODYNAMIC PULSATION MODELS OF RED GIANTS

Pulsation periods of the Mira-type star models were determined using the discrete Fourier transform of the kinetic energy of the limit-cycle stellar pulsation motions. The self-excited nonlinear stellar pulsations with transition to the limit-cycle oscillations were obtained as the solution of the Cauchy problem for equations of radiation hydrodynamics with initial conditions determined from selected hydrostatically equilibrium evolutionary models. Effects of time-dependent convection were taken into account by solution of the transport equations for diffusion of the specific enthalpy and the mean kinetic energy of turbulent motions (Kuhfuß(1986). Basic equations of hydrodynamics and parameters of the theory of time-dependent convection are described in (Fadeyev 2013).

A substantial difficulty encountered in pulsation calculations of Mira-type stars is due to the fact that the hydrostatically equilibrium stellar envelope might be in thermal imbalance whereas the thermal equilibrium is the necessary condition for application of the theory of stellar pulsation and for correct evaluation of the pulsation period (Ya’Ari and Tuchman 1996). To avoid this obstacle we used an approach based on evaluation of the degree of deviation from thermal equilibrium within the stellar envelope (Fadeyev 2022). To this end we evaluated the quantity

$$\delta_{\text{L}} = \max_{1 \leq j \leq N} |1 - L_j/L_1|,$$

where L_j is the radiative plus convective luminosity at the j -th mass zone of the hydrodynamic model. The inner boundary ($j = 1$) is treated as a rigid permanently radiating sphere and at the outer boundary $j = N$. All hydrodynamic computations were carried out with $N = 600$ mass zones. The condition $\delta_{\text{L}} = 0$ obviously corresponds to the thermal equilibrium. The criterion of enough small deviations from thermal equilibrium when the theory of stellar pulsation is

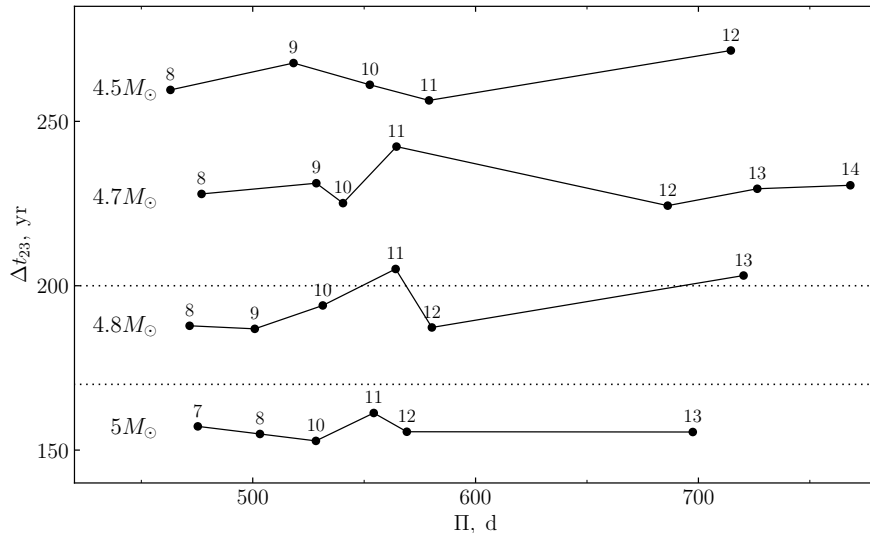


Figure 5. The diagram period Π — duration of the second phase of radius decrease Δt_{23} for evolutionary sequences $M_{\text{ZAMS}} = 4.5M_{\odot}$, $4.7M_{\odot}$, $4.8M_{\odot}$ and $5M_{\odot}$ computed for $\eta_{\text{B}} = 0.05$. Dotted lines show the time interval $170 \text{ yr} \leq \Delta t \leq 200 \text{ yr}$.

applicable is given by the condition $\delta_{\text{L}} \lesssim 10^{-2}$ (Fadeyev 2022). Computations carried out in the present study showed that this condition is fulfilled in vicinity of stellar radius extremums shown in Figs. 1 and 2 by filled circles.

The relationship between the duration of the first phase of radius decrease Δt_{01} and the pulsation period Π at the maximum of $L_{3\alpha}$ is shown in Fig. 4 for evolutionary sequences $M_{\text{ZAMS}} = 1.8M_{\odot}$ and $M_{\text{ZAMS}} = 2M_{\odot}$ computed with $\eta_{\text{B}} = 0.05$. Increase of pulsation period Π with increasing serial number of the thermal flash i_{TP} is due to the fact that the stellar luminosity and the radius at the maximum of $L_{3\alpha}$ gradually grow as the AGB star evolves. The time interval Δt_{01} gradually decreases with increasing i_{TP} and, therefore, with increasing pulsation period. As can be seen in Fig. 4, the pulsation periods of red giants with masses $M \lesssim 2M_{\odot}$ at the maximum of $L_{3\alpha}$ in general do not exceed 400 d and radial pulsations with periods $\Pi \approx 500$ d exist only during the final stage of AGB when the time interval Δt_{01} is less than 100 yr. Therefore, the assumption that the secular period reduction of R Hya takes place during the first phase of radius decrease should undoubtedly be rejected.

The diagram illustrating the relationship between the pulsation period and the time interval Δt_{23} shown in Fig. 5 allows us to conclude that an acceptable agreement between the theory and observations is obtained for the evolutionary sequence $M_{\text{ZAMS}} = 4.8M_{\odot}$. It should be noted that the non-monotonic change in time interval Δt_{23} with increasing i_{TP} is due to irregular variations of the maximum radius R_2 .

Table 1. Models of the Mira-type star R Hya with initial mass $M_{\text{ZAMS}} = 4.8M_{\odot}$

η_{B}	i_{TP}	M/M_{\odot}	$X_{\text{C}}/X_{\text{O}}$	Δt_{23} , yr	R_2/R_{\odot}	R_3/R_{\odot}	Π_2 , d	Π_3 , d
0.03	6	4.63	0.305	177	495	429	451	383
	7	4.60	0.331	164	512	437	469	387
	8	4.58	0.355	154	532	445	473	393
0.05	5	4.58	0.279	197	498	421	470	377
	6	4.54	0.302	173	502	429	473	389
	7	4.50	0.328	189	515	435	471	394
0.07	5	4.50	0.282	200	499	424	472	386
	6	4.44	0.306	177	506	433	463	398

MODELS OF THE MIRA-TYPE VARIABLE R HYA

Early observational estimates of the pulsation period of R Hya $\Pi_a \approx 495$ d obtained at the turn of XVIIth–XVIIIth centuries are scarce and rather unreliable (Zijlstra et al. 2002), so that computation of R Hya model should take into account the period value $\Pi_b \approx 380$ d corresponding to nearly 1950 when the period decrease ceased. To this end we computed additional evolutionary sequences of AGB stars with initial mass $M_{\text{ZAMS}} = 4.8M_{\odot}$ for the mass loss parameters $\eta_{\text{B}} = 0.03$ and $\eta_{\text{B}} = 0.07$. Selected models of these sequences corresponding to the second radius maximum R_2 and the second radius minimum R_3 were used as initial conditions in hydrodynamic computations and finally for determination of pulsation periods Π_2 and Π_3 .

Results of these computations are collected in table 1 for models with initial mass $M_{\text{ZAMS}} = 4.8M_{\odot}$, where in first four columns we give the mass loss parameter η_{B} (Blöcker 1995), the serial number of the thermal flash i_{TP} , the mass of the star at maximum of $L_{3\alpha}$ (i.e. for $t=0$) and the ratio of carbon ^{12}C to oxygen ^{16}O mass abundances at the outer boundary of the evolutionary model. It should be noted that at the early AGB stage prior to the first thermal pulse the surface ratio of mass abundances is $X_{\text{C}}/X_{\text{O}} = 0.248$ and therefore the composition of models listed in table 1 is characterized by the enhanced carbon abundance indicating the stage of the 3rd dredge-up. At the same time all the models remain the oxygen-rich Miras because the ratio of surface concentrations is $N_{\text{C}}/N_{\text{O}} < 1$.

All models listed in table 1 satisfy the condition that the pulsation period Π_3 differ from the observational estimate $\Pi_b^* = 380$ d by less than 5%.

CONCLUSIONS

Results of stellar evolution and nonlinear stellar pulsation calculations allow us to draw an unambiguous conclusion that the period decrease observed in R Hya corresponds to the second phase of radius decrease when the radiation–diffusion wave from the helium burning shell dissipates in the outer layers of the star. Earlier the same conclusion was drawn by Wood and Zarro (1981) on the basis of their evolutionary calculations. At the same time we have to note the significant difference between estimates of stellar parameters presented by Wood and Zarro (1981) and those obtained in our study. In particular, the mass of the carbon–oxygen degenerate core and the stellar luminosity of our model are $M_{\text{CO}} = 0.856M_{\odot}$ and $L \approx 2.5 \times 10^4 L_{\odot}$, whereas estimates obtained by Wood and Zarro (1981) are significantly smaller: $M_{\text{CO}} = 0.653M_{\odot}$, $L \approx 1.3 \times 10^4 L_{\odot}$. This disagreement is due to the fact that estimates by Wood and Zarro (1981) were obtained for the significantly longer phase of radius decrease and did not take into account the fact that the period of R Hya has ceased to decrease in ≈ 1950 .

R Hya is one of the nearby long–period pulsating variables and by now the measurements of its angular diameter were carried out with methods of the optical interferometry. According to Haniff et al. (1995) the angular diameter of R Hya is $d = 33$ mas and for the distance 125 pc its stellar radius is $R = 442R_{\odot}$. It should be noted that this distance estimate was obtained from the approximate period–luminosity–color relation (Feast et al. 1989). However the recent distance estimate based on the astrometric catalog Gaia DR3 is 126 pc (Andriantsaralaza et al. 2022) so that the observational estimate of the radius remains the same. Thus agreement of theoretical estimates of radii R_3 listed in table 1 with observations confirm the theoretical estimates of the stellar mass: $4.44M_{\odot} \leq M \leq 4.63M_{\odot}$. The range of mass estimates is less than 5%. This is not only due to variations of mass loss rate parameter η_{B} , but also due to computational accuracy limitations hampering a reliable evaluation of the maximum stellar radius R_2 .

REFERENCES

1. M. Andriantsaralaza, S. Ramstedt, W.H.T. Vlemmings, and E. De Beck, *Astron. Astrophys.* **667**, A74 (2022).
2. M. Asplund, N. Grevesse, A.J. Sauval, and P. Scott, *Annual Rev. Astron. Astrophys.* **47**, 481 (2009).
3. T. Blöcker, *Astron. Astrophys.* **297**, 727 (1995).

4. E. Böhm–Vitense, *Zeitschrift für Astrophys.* **46**, 108 (1958).
5. A.J. Cannon and E.C. Pickering, *Annals of Harvard College Observatory* **55**, 95 (1909).
6. S. C. Chandler, *Astron. Nachr.* **103**, 225 (1882).
7. R.H. Cyburt, A.M. Amthor, R. Ferguson, Z. Meisel, K. Smith, S. Warren, A. Heger, R.D. Hoffman, T. Rauscher, A. Sakharuk, H. Schatz, F.K. Thielemann, and M. Wiescher, *Astrophys. J. Suppl. Ser.* **189**, 240 (2010).
8. Yu.A. Fadeyev, *Astron. Lett.* **39**, 306 (2013).
9. Yu.A. Fadeyev, *MNRAS* **514**, 5996 (2022).
10. M.W. Feast, I.S. Glass, P.A. Whitelock, and R.M. Catchpole, *MNRAS* **241**, 375 (1989).
11. B.A. Gould, *Astron. Nachr.* **102**, 341 (1882).
12. C.A. Haniff, M. Scholz, and P.G. Tuthill, *MNRAS*, **276**, 640 (1995).
13. F. Herwig, *Astron. Astrophys.* **360**, 952 (2000).
14. F. Herwig, N. Langer, and M. Lugaro, *Astrophys. J.* 593, 1056 (2003).
15. D. Hoffleit, *J. Am. Associat. Var. Star Observ.* **25**, 115 (1997).
16. E.M.L. Humphreys, M.D. Gray, J.A. Yates, and D. Field, *MNRAS* **287**, 663 (1997).
17. M.J. Ireland, P.G. Tuthill, T.R. Bedding, J.G. Robertson, and A.P. Jacob, *MNRAS* **350**, 365 (2004).
18. R. Kuhfuß, *Astron. Astrophys.* 160, 116 (1986).
19. T. Lebzelter and J. Hron, *Astron. Astrophys.* **411**, 533 (2003).
20. B.M. Lewis, P. David P, and A.M. Le Squeren, *Astron. Astrophys. Suppl. Ser.* **111**, 237 (1995).
21. S.J. Little, I.R. Little–Marenin, and W.H. Bauer, *Astron. J.* **94**, 981 (1987).
22. H. Ludendorff, *Astron. Nachr.* **203**, 117 (1916).
23. H. Maehara, *Publ. Astron. Soc. Japan* **23**, 313 (1971).
24. P.W. Merrill, *Astrophys. J.* **103**, 6 (1946).
25. P.W. Merrill, *Publ. Astron. Soc. Pacific* **69**, 77 (1957).

26. R. Müller, *Astron. Nachr.* **237**, 81 (1929).
27. A.V. Nielsen, *Astron. Nachr.* **227**, 141 (1926).
28. M.Ya. Orlov and A.V. Shavrina, *Nauchn. Inform. Astron. Sovet AN SSSR* **56**, 97 (1984).
29. B. Paxton, R. Smolec, J. Schwab, A. Gaudy, L. Bildsten, M. Cantiello, A. Dotter, R. Farmer, J.A. Goldberg, A.S. Jermyn, S.M. Kanbur, P. Marchant, A. Thoul, R.H.D. Townsend, W.M. Wolf, M. Zhang, and F.X. Timmes, *Astrophys. J. Suppl. Ser.* **243**, 10 (2019).
30. M. Pignatari, F. Herwig, R. Hirschi, M. Bennett, G. Rockefeller, C. Fryer, F.X. Timmes, C. Ritter, A. Heger, S. Jones, U. Battino, A. Dotter, R. Trappitsch, S. Diehl, U. Frischknecht, A. Hungerford, G. Magkotsios, C. Travaglio, and P. Young, *Astrophys. J. Suppl. Ser.* **225**, 24 (2016).
31. D. Reimers, *Problems in stellar atmospheres and envelopes* (Ed. B. Baschek, W.H. Kegel, G. Traving, New York: Springer-Verlag, 1975), p. 229.
32. N.N. Samus', E.V. Kazarovets, O.V. Durlevich, N.N. Kireeva, and E.N. Pastukhova, *Astron. Rep.* **61**, 80 (2017).
33. J.F.J. Schmidt, *Astron. Nachr.* **65**, 173 (1865).
34. H. Takaba, I. Takahiro, M. Takeshi, and S. Deguchi, *Publ. Astron. Soc. Japan* **53**, 517 (2001).
35. P.R. Wood and D.M. Zarro, *Astrophys. J.* **247**, 247 (1981).
36. H.C. Woodruff, P.G. Tuthill, J.D. Monnier, M.J. Ireland, T.R. Bedding, S. Lacour, W.C. Danchi, and M. Scholz, *Astrophys. J.* **673**, 418 (2008).
37. A. Ya'Ari and Y. Tuchman, *Astrophys. J.* **456** 350 (1996).
38. A.A. Zijlstra, T.R. Bedding, and J.A. Mattei, *MNRAS* **334**, 498 (2002).